EPA Public Access
Author manuscript
J Exp Mar Bio Ecol. Author manuscript; available in PMC 2019 July 11.
About author manuscripts | Submit a manuscript

Published in final edited form as:
J Exp Mar Bio Ecol. 2018 ; 21: 466–472. doi:10.1016/j.jembe.2018.07.006.

Nitrogen uptake and allocation estimates for *Spartina alterniflora* and *Distichlis spicata*

Troy D. Hill[a,*], **Nathalie R. Sommer**[b], **Caroline R. Kanaskie**[c], **Emily A. Santos**[d], and **Autumn J. Oczkowski**[a]

[a]United States Environmental Protection Agency, Office of Research and Development, 27 Tarzwell Drive, Narragansett, RI 02882, United States

[b]Yale University, School of Forestry and Environmental Studies, 205 Prospect Street, New Haven, CT 06511, United States

[c]University of New Hampshire, Department of Natural Resources and the Environment, 46 College Road, Durham, NH 03824, United States

[d]Humboldt State University, College of Natural Resources and Sciences, 1 Harpst Street, Arcata, CA, 95521, United States

Abstract

Salt marshes have the potential to intercept nitrogen that could otherwise impact coastal water quality. Salt marsh plants play a central role in nutrient interception by retaining N in above- and belowground tissues. We examine N uptake and allocation in two dominant salt marsh plants, short-form *Spartina alterniflora* and *Distichlis spicata*. Nitrogen uptake was measured using ^{15}N tracer experiments conducted over a four-week period, supplemented with stem-level growth rates, primary production, and microbial denitrification assays. By varying experiment duration, we identify the importance of a rarely-measured aspect of experimental design in ^{15}N tracer studies. Experiment duration had a greater impact on quantitative N uptake estimates than primary production or stem-level relative growth rates. Rapid initial scavenging of added ^{15}N caused apparent nitrogen uptake rates to decline by a factor of two as experiment duration increased from one week to one month, although each experiment shared the qualitative conclusion that *Distichlis* roots scavenged N approximately twice as rapidly as *Spartina*. We estimate total N uptake into above- and belowground tissues as 154 and 277 mg $N \cdot m^{-2} \cdot d^{-1}$ for *Spartina* and *Distichlis*, respectively. Driving this pattern were higher N content in *Distichlis* leaves and belowground tissue and strong differences in primary production; *Spartina* and *Distichlis* produced 8.8 and 14.7 g $biomass \cdot m^{-2} \cdot d^{-1}$. Denitrification potentials were similar in sediment associated with both species, but the strong species-specific difference in N uptake suggests that *Distichlis*-dominated marshes are likely to intercept more N from coastal waters than are short-form *Spartina* marshes. The data and source code for this manuscript are available as an R package from https://github.com/troyhill/NitrogenUptake2016.

*Corresponding author: 1-401-782-3146, hill.troy@gmail.com.

5. Data statement

Data and source code used in this study are available as an R package hosted on GitHub (https://github.com/troyhill/NitrogenUptake2016), permanently archived by Zenodo (DOI: 10.5281/zenodo.1226378) and described in Hill et al. (Submitted).

EPA Author Manuscript
EPA Author Manuscript
EPA Author Manuscript

EPA Author Manuscript

EPA Author Manuscript

EPA Author Manuscript

Keywords

nitrogen uptake; nitrogen-15; salt marsh; *Spartina alterniflora*; *Distichlis spicata*

1. Introduction

Nitrogen (N) enrichment in coastal ecosystems is a chronic and widespread phenomenon (Paerl et al., 2002), and one that may be exacerbated by changing precipitation regimes (Sinha et al., 2017). Salt marshes occur along terrestrial margins and serve as buffers, retaining and transforming N before it reaches coastal waters (Craft et al., 2009) and can contribute to cultural eutrophication. The N-buffering capacity of salt marshes reflects the combined effects of microbial conversion of N to gaseous forms, sediment accumulation, and plant uptake of mineral N into organic tissues.

Microbial denitrification converts bioavailable forms of N to less reactive gaseous compounds (e.g., Koop-Jakobsen and Giblin, 2010; Yang et al., 2015) that can be readily exported to the atmosphere. The magnitude of denitrification is estimated at ~25% of annual plant N demand (White and Howes, 1994). Burial of N in deposited mineral sediment is a function of cation exchange capacity and sediment accumulation rates, both of which are variable and potentially impermanent (Anisfeld and Benoit, 1997). Nitrogen is also taken up by plants and stored in organic tissue during the growing season, when it is, in roughly equal parts, released to coastal waters or translocated to belowground plant structures for future re-use (Hopkinson and Schubauer, 1984) or long-term burial in dead organic tissues (White and Howes, 1994). This understanding of plant N cycling suggests that approximately half of annual plant N demand is supplied by inorganic N imported in coastal waters or produced by local N fixation.

In salt marshes from the northeastern United States to the Gulf Coast, short-form *Spartina alterniflora* Loisel and *Distichlis spicata* (L.) Greene (hereafter *Spartina* and *Distichlis*) can co-occur and behave as dominants on the marsh platform. Both species are typically N-limited (Smart and Barko, 1980) and respond positively to N enrichment throughout their ranges, increasing their biomass and dominance (Levine et al., 1998; Pennings et al., 2002). To the extent that these species differ in N uptake capacity, environmental changes affecting their dominance may have ancillary effects on ecosystem-scale nutrient interception.

Nutrient enrichment itself can affect competition between these species, potentially signaling disparate N uptake capacities. Community ecology theory suggests that relief from nutrient limitation may lead to *Spartina* to outcompete *Distichlis*, as competition shifts from nutrients to light (Levine et al., 1998). However, nutrient enrichment experiments have shown *Distichlis* increasing in dominance at the expense of *Spartina* (Fox et al., 2012; Pennings et al., 2002). The nature of the changing N regime - whether additional N is delivered as a “press” through a rising baseline level or in episodic pulses - may also play a role in enrichment effects on species cover and the ability of marsh plants to capture N. Understanding N uptake dynamics in these two species may provide insight into competitive outcomes under eutrophic conditions, and can provide a basis for estimating the nutrient-interception implications of shifts in dominance, regardless of cause.

EPA Author Manuscript EPA Author Manuscript EPA Author Manuscript

The use of ^{15}N as a tracer is a common means of investigating N uptake dynamics. This approach is particularly useful when N stocks are poorly constrained or where production and N uptake may be loosely coupled. As a methodological tool ^{15}N is powerful, but cost and labor requirements often limit applications to a single time interval. Time periods used for ^{15}N studies vary widely, from two days (Mozdzer et al., 2014) to three months (Oczkowski et al., 2015) to as much as seven years (White and Howes, 1994). Because uptake rates are calculated based on the amount of ^{15}N accumulated and the time elapsed, tracer studies using different time intervals have differential sensitivity to temporal variation in N uptake, and at least over long time periods emphasize different processes, as initial plant-microbe competition gives way to translocation dynamics and leaching rates (White and Howes, 1994).

We conducted a ^{15}N tracer study to improve our understanding of N capture and allocation by *Spartina* and *Distichlis*, and to optimize the application and interpretation of ^{15}N tracer methods. Our first objective was to quantify N uptake and allocation to above- and belowground tissues over a one-month time scale. Based on a zonation paradigm in which plants occupying less stressful, higher-elevation areas more efficiently compete for nutrients (Levine et al., 1998), we hypothesized that *Distichlis* would scavenge N more efficiently than *Spartina*. We further hypothesized that in both species, N would be partitioned rapidly into aboveground photosynthetic tissues. Our second objective was to test the importance of potential determinants of N capture. The determinants we considered were relative growth rates of individual shoots, primary production, root biomass, and experiment duration. We hypothesized that shoot growth rates and root biomass will be critical determinants of N uptake, respectively mediating demand for, and access to, dissolved N.

2. Material and methods

2.1. Experimental design

On 21 June 2016, vegetated salt marsh cores (hereafter “mesocosms”) were collected from Colt State Park in Bristol, RI. Mesocosms were collected by inserting modified polyvinylchloride (PVC) coring tubes (35 cm × 10 cm dia.) into the marsh platform. Live aboveground biomass was protected from damage during retrieval using PVC extensions. After extracting the mesocosms from the marsh, mesh netting (0.5 mm) was secured to the bottom of the PVC to prevent sediment loss during the experiment. A total of 30 mesocosms were collected, 15 each from monoculture areas of short-form *Spartina* and *Distichlis* at similar elevations on the marsh platform.

Following collection, mesocosms were transferred to a tidal basin (0.6 m × 1 m dia.) located in an outdoor greenhouse at the US Environmental Protection Agency’s Atlantic Ecology Division. Semidiurnal tides were simulated with seawater pumped from Narragansett Bay and timer-operated solenoid valves at the input and outlet of the basin. Using the same system described by Hanson et al. (2016), the water level in the tidal basin was gradually raised from low tide (0.20 m) to high tide (0.45 m; determined by a standpipe) over a four-hour period beginning when the input solenoid was opened at 5 a.m. each morning. Flood tide was followed by a two hour slack tide when the input solenoid was closed, a four hour period of ebb tide drainage (drain solenoid opened), and a two hour slack low tide before the

EPA Author Manuscript

EPA Author Manuscript

EPA Author Manuscript

cycle began again. Mesocosms were positioned on a grate to allow drainage, and were inundated to a depth of 0.05 m during high tides. Mesocosms were redistributed inside the tidal basin every three days to homogenize exposure to ambient sunlight.

2.2. Allometry and aboveground production

Every live culm in each mesocosm was tagged and heights were measured to the nearest millimeter on 22 June, 29 June, 6 July, 13 July, and 20 July 2016. Stem heights were also recorded for mesocosms as they were harvested. New shoots were tagged throughout the experiment, and in total 839 unique shoots were tracked. Stem densities were calculated directly from counts of live shoots, and shoot masses were estimated from heights using species-specific allometry equations developed for the marsh where mesocosms were initially collected.

Allometric models were developed from live shoots collected from Colt State Park in May, June, and July 2016. At each sampling event, three 25 × 25 cm quadrats were collected from monoculture areas of short-form *Spartina* and *Distichlis*. Stems were cut at the sediment surface, measured to the nearest millimeter, and a representative subsample of stems were individually dried to constant weight at 50°C. Masses were modeled as a function of height following Lu et al. (2016), with linear models parameterized using Box-Cox power transformations of biomass (λ) selected to maximize normality of residuals (Box and Cox, 1964). Species-specific allometry equations took the form $mass = e^{(height \cdot a + b)}$ for $\lambda = 0$, and $mass = (height \cdot a + b)^{1/\lambda}$ for $\lambda \neq 0$ (Box and Cox, 1964). These allometry equations were applied to the stem height measurements collected in the greenhouse experiment. Net aboveground primary production (NAPP) was calculated for each mesocosm as the sum of positive live biomass increments at the mesocosm-scale (Milner and Hughes, 1968).

The performance of allometry models was evaluated by comparing predicted biomass with biomass directly measured during mesocosm harvests. By this measure, allometry-based biomass estimates averaged 31 $g \cdot m^{-2}$ (14%) higher than the total observed biomass (Hill et al. (Submitted)). Although the absolute magnitude of the errors was similar between species, the lower total biomass in *Spartina* mesocosms increased the proportional error, making *Distichlis* allometry models more accurate by this measure (8% vs. 19% error).

Estimated shoot masses were used to calculate relative growth rates (RGR; $g \cdot g^{-1} \cdot d^{-1}$); the rate of biomass accumulation per unit of biomass. RGR was calculated for each tagged shoot as the difference between sequential log-transformed shoot masses (M_{t-1} and M_t in eq. 1) divided by the time interval between measurements (Hunt, 1990). For shoot i over the time period T_{t-1} to T_t, RGR was calculated as:

$$RGR_{i_t} = \frac{\ln(M_{i_t}) - \ln(M_{i_{t-1}})}{T_t - T_{t-1}} \quad \text{eq. 1}$$

RGR was averaged across all unique stems in each mesocosm. When multiple growth rate measurements were available for an individual shoot, they were averaged to get a single representative quantity for each unique shoot, before calculating a mesocosm average.

EPA Author Manuscript

EPA Author Manuscript

EPA Author Manuscript

2.3. ^{15}N tracer pulse

To track N uptake, we added ^{15}N tracer to each mesocosm using a solution of 99 atom percent $K^{15}NO_3$ in artificial seawater. During an ebb tide on 24 June 2016, 4 mL of tracer solution was injected into the sediment at three evenly-spaced points in each mesocosm, adding a combined 1.95 mg ^{15}N to each mesocosm. Mesocosms grown in the greenhouse received the single dose of ^{15}N tracer at the same time, but were deconstructed over the subsequent month, as described below, allowing variable amounts of time for ^{15}N movement and allocation.

The ^{15}N application used in this study is equivalent to a one-time addition of 246 mg $N \cdot m^{-2}$ (243 mg $^{15}N \cdot m^{-2}$), large enough to enable detection of plant uptake and allocation while minimally affecting the soil N stock. Our interpretation assumes that the tracer application did not introduce enough total N to cause enrichment artifacts, and that our study represents the response of wetlands in an ambient N regime to a small pulse. Although we did not test this assumption, our N loading rate is low relative to literature values from studies in ambient nutrient regimes (Table S1).

2.4. Mesocosm processing

At collection (21 June 2016) and at weekly intervals beginning nine days after tracer addition, a cohort of three randomly selected mesocosms from each species was harvested for analysis of ^{15}N accumulation in above- and belowground tissue. This sampling occurred on 1 July, 8 July, 15 July, and 22 July 2016. Above-ground biomass was clipped at the sediment surface, rinsed with deionized water and separated into live and standing dead biomass. Live biomass was further separated into stems, dead leaves, and live leaves. Live leaves were separated by position relative to the top of the shoot, although these node-level data were pooled together during data analysis.

After aboveground biomass was sampled, peat was extruded from the coring tube and sectioned into six depth intervals: 0–2 cm, 2–5 cm, 5–10 cm, 10–15 cm, 15–20 cm, and 20–30 cm. Surface litter and algal mat layers were separated when present. Each depth interval was subsampled for belowground biomass and bulk density. One quarter of each depth interval volume was dried to constant weight at 50°C, with bulk density calculated as the bulk sediment dry mass divided by the sample volume. One quarter of each depth interval was archived in a freezer, and the remaining half of each depth interval was used for separation of belowground biomass. Within one week of harvest, belowground biomass was rinsed clean of sediment using deionized water and separated into live rhizomes, live coarse roots (>1 mm), live fine roots (≤1 mm), and dead biomass. Live biomass was distinguished from dead by its white color and turgid structure. All samples were dried to constant weight at 50°C, ground using a Wiley mill using a size 40 screen, and stored in acid-washed scintillation vials. Enriched and unenriched samples were ground on separate mills to prevent contamination.

2.5. Potential and *in vitro* denitrification

On 9 July 2016 two acetylene inhibition assays were conducted using subsamples of 0–5 cm depth intervals from each of the six mesocosms harvested the previous day. Denitrification

EPA Author Manuscript EPA Author Manuscript EPA Author Manuscript

enzyme activity (DEA) potential was measured by incubating 6.5 g of sediment in 70 mL jars sealed with rubber septa. Sample containers were amended with 12 mL of nutrient-amended filtered seawater (7 mmol N L^{-1} as KNO_3; 17 mmol C L^{-1} as D-glucose; and 6 mmol P L^{-1} as KH_2PO_4) with 0.125 g L^{-1} chloramphenicol added as a microbial inhibitor. Containers were alternately evacuated and flushed with N_2 three times, and acetylene (10% of headspace volume) was added to block reduction of N_2O to N_2. *In vitro* denitrification was measured in nearly identical acetylene inhibition assays. The only difference was the use of unamended filtered seawater rather than a nutrient solution, following Warneke et al. (2011). *In vitro* denitrification and DEA assays estimate microbial denitrification under ambient conditions, wherein some compound may be limiting, and after removing limitation. These measures therefore provide reasonable lower and upper-bound estimates of denitrification.

In both assays, N_2O accumulation in the jars was measured at 30 minute intervals over a period of two hours, with 5 mL of sample headspace and 10 mL of N_2 transferred to evacuated 12 mL exetainers (Labco, UK). Sampled headspace was replaced with a 10% mixture of acetylene in N_2. Nitrous oxide concentrations were analyzed by gas chromatography (GC; Shimadzu GC2014) using an electron capture detector (ECD). The GC column oven temperature was 75°C, the ECD temperature was 325°C, the carrier gas was helium and makeup gas was a 5% solution of methane in argon. Potential and *in vitro* denitrification were measured as the slope of the line of best fit for dilution-corrected N_2O concentrations in the jar headspace. At least three points were used for each rate estimate, and all relationships had $R^2 \geq 0.92$ (mean $R^2 = 0.97$). A laboratory blank using DEA solution and no added sediment yielded zero flux (slope = 0.0; $R^2 = 0.0$), so no blank correction was applied. Fluxes per gram of bulk sediment were divided by the sediment inventory (g m^{-2}) to express gas fluxes per unit area, units comparable to N uptake rates.

2.6. Analytical measurements and N uptake calculations

Nitrogen concentrations and isotope ratios were measured using an Elementar Vario Micro elemental analyzer connected to a continuous flow Isoprime 100 isotope ratio mass spectrometer (Elementar Americas, Mt. Laurel, NJ). Check standards, blanks, and sample replicates were run every ten samples. Replicate analyses of isotopic standard reference materials USGS 40 ($\delta^{13}C = -26.39$ ‰; $\delta^{15}N = -4.52$ ‰) and USGS 41 ($\delta^{13}C = 37.63$ ‰; $\delta^{15}N = 47.57$ ‰) were used to normalize isotopic values of working standards to the Air ($\delta^{15}N$) and Vienna Pee Dee Belemnite ($\delta^{13}C$) scales (Paul et al., 2007). Average recoveries for standard reference materials were ±1.1% for $\delta^{15}N$, ±0.4% for total N, ±0.03% for $\delta^{13}C$, and ±0.05% for total C. Coefficients of variation on sample replicates averaged 8.9% for $\delta^{15}N$, 5.9% for total N, −0.5% for $\delta^{13}C$, and 3.6% for total C.

Isotope composition reported by the mass spectrometer is in per mil notation, where $\delta^{15}N = [(R_{sample}\text{-}R_{air})/R_{air}] \times 10^3$. This was converted to atom-percent notation as:

$$^{15}N \quad AP = \frac{\delta^{15}N + 1000}{\delta^{15}N + 1000 + (1000 \div 0.0036765)} \times 100 \quad \text{eq. 2}$$

EPA Author Manuscript

EPA Author Manuscript

EPA Author Manuscript

The mass of ^{15}N recovered was calculated in two steps. First, the atom percent (AP) excess ^{15}N ($^{15}N_{xs}$) was calculated for each sample by subtracting the background ^{15}N AP for each compartment (based on time-zero data) from ^{15}N AP in enriched samples. An additional correction was applied to belowground biomass; $^{15}N_{xs}$ in dead biomass was subtracted from live biomass compartments to account for sorption of ^{15}N to organic matter and focus on incorporation of ^{15}N into tissue (Mozdzer et al., 2014). Multiplying $^{15}N_{xs}$ by the percent N and total biomass in the associated compartment provides the ^{15}N mass recovered, which can be directly compared to the mass of tracer added.

Aboveground N uptake was estimated independently using ^{15}N and harvest techniques. Rates of ^{15}N uptake (mg $^{15}N \cdot m^{-2} \cdot d^{-1}$) were calculated using the mass of ^{15}N recovered in live aboveground tissue and the time elapsed between tracer addition and harvest. In the harvest technique, total N uptake was estimated by multiplying primary production rates by a weighted average of N content in aboveground tissues.

2.7. Belowground primary production

In the absence of direct measurements of net belowground primary production (NBPP), we estimated NBPP and N uptake using $^{15}N_{xs}$ accumulation and the stoichiometry of belowground tissue. When a significant relationship was observed between aboveground $^{15}N_{xs}$ uptake and total N uptake estimated from aboveground production, the relationship between the two measures ($TN_{AG} = {}^{15}N_{AG} \times a_{AG} + b_{AG}$) was applied to belowground $^{15}N_{xs}$ uptake rates ($^{15}N_{BG}$; mg $^{15}N \cdot m^{-2} \cdot d^{-1}$) to estimate total N accumulation in belowground tissue (TN_{BG}; mg $N \cdot m^{-2} \cdot d^{-1}$; eq. 3). The stoichiometry of belowground tissue was then used to estimate biomass production required for a given total N uptake rate (eq. 4). Specifically, belowground N uptake rates were divided by the weighted-average N concentration in belowground tissues to estimate belowground biomass production (mg biomass $\cdot m^{-2} \cdot d^{-1}$):

$$TN_{BG} = {}^{15}N_{BG} \times a_{AG} + b_{AG} \quad \text{eq. 3}$$

$$NBPP = TN_{BG} \div \frac{mg\ N}{mg\ biomass} \quad \text{eq. 4}$$

This approach makes two important assumptions. First, it assumes that above- and belowground tissues do not differentially discriminate between ^{15}N and ^{14}N. Assuming no fractionation differences between tissues means that $^{15}N_{xs}$ accumulation is similarly representative of total N accumulation in both tissues, and allows model parameters a_{AG} and b_{AG} to be applied to belowground ^{15}N uptake to estimate total N uptake. Secondly, this approach assumes that the bulk of $^{15}N_{xs}$ measured in roots and rhizomes is incorporated into tissues and reflects production. $^{15}N_{xs}$ in live roots and rhizomes was corrected for sorption by subtracting $^{15}N_{xs}$ in dead biomass, but we did not measure and cannot correct for ^{15}N that was in the process of translocation to aboveground tissue.

EPA Author Manuscript

EPA Author Manuscript

EPA Author Manuscript

2.8. Statistical analysis

Temporal trends in biomass and N content were evaluated for each species using linear models. Statistical comparisons of mean values between species were made using Welch's t-test, with non-integer degrees of freedom rounded down. Differences between species and the effect of experiment duration (four weekly harvests following a single ^{15}N application) on N uptake rates were evaluated using two-way analysis of variance (ANOVA) with species and time as main effects. Potentially important controls on total (above- and belowground) ^{15}N uptake were evaluated using species-specific multiple regression models with experiment duration, relative growth rates, primary production, and root biomass as explanatory variables. All analyses were conducted in R version 3.5.1.

3. Results

3.1. Stem allometry, aboveground biomass and production

Stem allometry was based on 95 *Distichlis* samples and 75 *Spartina* stems collected from Colt State Park, RI. These data suggest strong species-specific differences in allometry. On the marsh platform, *Distichlis* had greater maximum stem heights than *Spartina* (Fig. 1), although *Spartina* generally weighed more at stem heights taller than 15 cm. Power transformations differed between the species and the resulting allometry parameters (Table 1) are not directly comparable, although Figure 1 suggests that *Spartina* has a more concave relationship between mass and height, indicating a more rapid increase in biomass per increment of shoot height. As a result, *Spartina* shoots tend to have a similar or higher mass than *Distichlis* shoots of the same height.

Cohorts varied in their initial standing aboveground biomass (Fig. 2), but biomass in all cases increased over time indicating steady primary production. Over the four harvests *Spartina* NAPP averaged 3.7 ± 0.56 $g \cdot m^{-2} \cdot d^{-1}$ and remained constant over time ($P = 0.14$), while *Distichlis* NAPP (pooled mean: 5.7 ± 0.99 $g \cdot m^{-2} \cdot d^{-1}$) increased over time ($R^2 = 0.64$, $F_{(1, 10)} = 20.4$, $P < 0.01$) and was significantly higher than *Spartina* during the third (Welch's two-sample t-test; $t_{(3)} = 4.6$, $P < 0.05$) and fourth ($t_{(3)} = 4.2$, $P < 0.05$) harvests (Fig. 3A).

3.2. Leaf and stem biomass, N stocks, and uptake

The time trend in leaf mass varied by species, with *Distichlis* leaf mass remaining constant and *Spartina* leaf mass declining slightly over the course of the experiment ($R^2 = 0.29$, $F_{(1,13)} = 6.6$, $P < 0.05$). Nonetheless, the species did not significantly differ in the amount of leaf biomass present (*Distichlis* and *Spartina* pooled means: 108 ±11 $g \cdot m^{-2}$ vs. 120 ±12 $g \cdot m^{-2}$; $P = 0.45$). Linear models of leaf N content over time showed no trend for either species ($P = 0.70$ and 0.18 for *Spartina* and *Distichlis*), but leaf N was consistently higher in *Distichlis* than *Spartina* (2.32 ±0.03% vs. 1.76 ±0.07%; $t_{(20)} = 7.1$, $P < 0.001$).

Similar trends were observed in stem tissue dynamics during mesocosm harvests. *Spartina* stem biomass declined slightly over time ($R^2 = 0.50$, $F_{(1, 13)} = 15$, $P < 0.01$) while *Distichlis* showed no trend ($P = 0.69$). Combining all cohorts, the two species differed significantly in the amount of stem biomass recovered ($t_{(23)} = 7.9$, $P < 0.001$), with *Distichlis* stem mass substantially higher than *Spartina* (227 ±16 $g \cdot m^{-2}$ vs. 83 ±10 $g \cdot m^{-2}$). There were no

EPA Author Manuscript

EPA Author Manuscript

EPA Author Manuscript

differences or time trends in stem N content (pooled mean: 1.14 ±0.04%), but the dramatic difference in mass led *Distichlis* mesocosms to consistently have a larger stem N stock (2.46 ±0.16 $g \cdot m^{-2}$ vs. 0.93 ±0.09 $g \cdot m^{-2}$; $t_{(21)} = 8.2$, $P < 0.001$).

The weighted average of N concentrations in leaves and stems was multiplied by the rate of primary production to estimate total N accumulation rates in aboveground biomass. Weighted average N concentrations did not vary over time for either species ($P = 0.06$ and 0.14 for *Spartina* and *Distichlis*) and both species had similar weighted average N concentrations ($P = 0.63$; pooled mean: 1.50 ±0.04% N). Nonetheless, mesocosm-specific weighted average N concentrations were used to estimate N uptake.

As a product of NAPP and tissue N, aboveground N uptake (mg $N \cdot m^{-2} \cdot d^{-1}$; Fig 3B) reflected the relatively stronger trends in NAPP. Nitrogen uptake was highly variable during the first harvest, possibly a result of the brief time period considered (7 days). Neither species had a systematic trend in total N uptake rates over time ($P = 0.24$ and 0.21 for *Spartina* and *Distichlis*). Across all mesocosms, mean N uptake rates were similar for both species ($P < 0.13$) and averaged 57.8 ±10.1 mg $N \cdot m^{-2} \cdot d^{-1}$ for *Spartina* and 85.7 ±14.8 mg $N \cdot m^{-2} \cdot d^{-1}$ for *Distichlis*. The two species differed in total N uptake only during the third ($t_{(2)} = 4.2$, $P < 0.05$) and fourth harvests ($t_{(3)} = 3.6$, $P < 0.05$). In both cases *Distichlis* accumulated N more rapidly than *Spartina* (Fig. 3B).

3.3. Belowground biomass and N stocks

Spartina fine root biomass declined over the four weeks of the study from ~325 $g \cdot m^{-2}$ to 142 $g\ m^{-2}$ ($F_{(1,13)} = 8.9$, $r^2 = 0.36$, $P < 0.05$). *Distichlis* fine root mass did not have a systematic time trend but was consistently lower than *Spartina* ($t_{(14)} = -4.7$, $P < 0.001$), averaging 75 ±4 $g \cdot m^{-2}$ vs. 205 ±27 $g \cdot m^{-2}$. Strong differences in N concentrations favored *Distichlis* (0.98 ±0.02% vs. 0.81 ±0.03%; $t_{(24)} = 5.5$, $P < 0.001$) but were insufficient to compensate for the much greater mass of *Spartina* fine roots, which led *Spartina* to have a larger fine root N stock (1.7 ±0.25 g $N \cdot m^{-2}$ vs. 0.73 ±0.04 g $N \cdot m^{-2}$; $t_{(14)} = -3.7$, $P < 0.01$).

Coarse root biomass was similar across species (126 ±16 $g \cdot m^{-2}$ for *Distichlis* vs. 168 ±17 for *Spartina*; $P = 0.09$) and through time. Despite significantly higher N content in *Distichlis* coarse roots (0.92 ±0.03% vs. 0.68 ±0.03%; $t_{(27)} = 6.2$, $P < 0.001$), coarse root N stocks were similar in both species (1.1 ±0.1 g $N \cdot m^{-2}$; $P = 0.87$).

Rhizomes were the dominant contributor to belowground biomass. Rhizome biomass did not vary over time, and *Distichlis* had twice as much rhizome biomass than *Spartina* (913 ±48 $g \cdot m^{-2}$ vs. 408 ±39 $g \cdot m^{-2}$; $t_{(26)} = 8.2$, $P < 0.001$). As observed in fine and coarse roots, *Distichlis* rhizomes had higher N content than *Spartina*, 0.85 ±0.03% vs. 0.65 ±0.03% ($t_{(27)} = 5.3$, $P < 0.001$). Although rhizomes had the lowest N content of any tissue type, their mass dominance made rhizomes the largest belowground N stock for both species. The rhizome N stock in *Distichlis* mesocosms averaged 7.7 ±0.44 g $N \cdot m^{-2}$, almost three times the 2.6 ±0.22 g $N \cdot m^{-2}$ stored in *Spartina* rhizomes ($t_{(20)} = 10.5$, $P < 0.001$).

EPA Author Manuscript

EPA Author Manuscript

EPA Author Manuscript

Belowground primary production was estimated from ^{15}N data as described in equations 3 and 4. The resultant estimates of belowground production averaged 6.6 and 8.1 g m^{-2} d^{-1} for *Spartina* and *Distichlis* (Table 3).

3.4. ^{15}N recoveries and N uptake estimates

Total ^{15}N recovered in the mesocosms, including in dead biomass and surficial algae, averaged 54% (Fig. 4). Although our tracer was added directly to porewater, 46% of the tracer added was unaccounted for at harvest. This quantity did not change over time, suggesting that the unaccounted-for ^{15}N was either unrelated to time-dependent processes such as denitrification, or that competition between plants and microbes for the added ^{15}N ended early in the experiment. Because the mesocosms were not closed systems, ^{15}N may also have been exported during tidal exchange.

Several differences were observed in ^{15}N allocation by the two species. *Spartina* had higher ^{15}N content in leaves ($t_{(19)} = -2.5$, $P < 0.05$), stems ($t_{(21)} = -3.0$, $P < 0.01$), and rhizomes (Table 2; $t_{(20)} = -2.3$, $P < 0.05$), while *Distichlis* had higher ^{15}N content in fine roots ($t_{(21)} = 2.2$, $P < 0.05$). When compartments were aggregated, *Spartina* had higher ^{15}N content in both above ($t_{(21)} = -2.9$, $P < 0.01$) and belowground tissues ($t_{(21)} = -2.2$, $P < 0.05$).

Similar masses of ^{15}N were recovered in the leaves and coarse roots of the two species, but differences were observed in the other compartments (Table 2). Compared with *Spartina, Distichlis* had more ^{15}N mass recovered in stems ($t_{(15)} = 5.2$, $P < 0.01$) and rhizomes ($t_{(15)} = 2.6$, $P < 0.05$), and less recovered in fine roots ($t_{(20)} = -2.5$, $P < 0.05$). These differences led *Distichlis* to have higher total ^{15}N recovery than *Spartina* ($t_{(19)} = 2.5$, $P < 0.05$; Table 2). Aboveground biomass captured more ^{15}N than belowground biomass in both species ($F_{(1,44)} = 12.7$, $P < 0.001$; partition main effect in two-way ANOVA), and *Distichlis* captured more ^{15}N than *Spartina* ($F_{(1,44)} = 6.9$, $P < 0.05$; species main effect).

Belowground ^{15}N data were corrected for abiotic sorption to biomass by subtracting ^{15}N adsorbed to dead peat in each mesocosm section. The sorption contribution to ^{15}N enrichment averaged 0.043 atom percent above natural background levels, compared with average sorption-corrected root and rhizome enrichment of 0.26 atom percent. There was no difference in sorption between species ($P = 0.56$), or substantial change over time ($P = 0.89$), emphasizing the role of dead organic matter as a medium-term reservoir for dissolved N.

When standardized to fine root biomass, ^{15}N uptake rates varied by species (ANCOVA: $F_{(1,20)} = 16$, $P < 0.001$) and with experiment duration ($F_{(1,20)} = 10$, $P < 0.01$; Fig. 5), with an insignificant interaction term ($F_{(1,20)} = 3$, $P = 0.12$). Mass-specific uptake rates declined as experiment duration increased, but were higher for *Distichlis*. ANCOVA did not detect a significant difference in slopes, but regression lines for the two species suggest an intersection would occur around day 46, at which point no difference in root-specific ^{15}N uptake would be observed.

Multiple regression analysis of potentially important controls on live-biomass ^{15}N uptake used experiment duration, mean relative growth rate of individual stems, mesocosm-scale primary production rates, and root biomass as explanatory variables in species-specific

EPA Author Manuscript

EPA Author Manuscript

EPA Author Manuscript

models. Both models had high explanatory power (*Spartina*: $F_{(4,7)} = 6$, $P < 0.05$, adj. $R^2 = 0.64$; *Distichlis*: $F_{(4,7)} = 5$, $P < 0.05$, adj. $R^2 = 0.59$), and in each case experiment duration was the only significant predictor of ^{15}N uptake ($P < 0.05$; partial $r^2 = 0.52$ and 0.64 for *Spartina* and *Distichlis*).

Although there is a strong temporal effect on rates of ^{15}N uptake, on time scales greater than three weeks there was general agreement between ^{15}N accumulation in aboveground biomass and estimates of total N uptake from biomass production (Fig. 6). To increase the power of the model, *Spartina* and *Distichlis* were pooled together in this analysis, making the assumption that their fractionation behavior (the relationship between ^{15}N uptake and total N uptake) is similar. The relationship between these two measures suggests that ^{15}N accumulation in tissue may be a useful indicator of total N uptake, at least on time scales of approximately a month.

3.5. Denitrification enzyme activity and total N interception

Denitrification enzyme activity, measured two weeks after the ^{15}N addition, was comparable in both species (Table 3; $P = 0.45$). Unamended gaseous N fluxes also did not differ between species ($P = 0.32$). Both processes were highly variable; standard errors ranged from 12–58% of the mean value. This is indicative of high spatial variation on the marsh platform.

Total N interception was estimated by combining our more integrative, longer-term estimates of N uptake into above- and belowground plant biomass (using data for 3–4 weeks after spike addition) with the potential for microbial N removal (DEA). Total plant and microbial N interception by *Distichlis* mesocosms (277.0 ± 25.5 mg N m^{-2} d^{-1}) was significantly higher than *Spartina* mesocosms (154.3 ± 11.8 mg N m^{-2} d^{-1}; $t_{(7)} = 4.4$, $P < 0.01$), due to higher aboveground production and N uptake by *Distichlis* (Table 3).

4. Discussion

4.1. ^{15}N uptake and N interception

Over a four-week tracer experiment, *Distichlis* consistently absorbed more N per gram of fine root biomass than *Spartina*. However, quantitative estimates of uptake rates declined by a factor of two as time passed. Dead organic matter appeared to serve as a reservoir that sorbed ^{15}N and may have enabled *Spartina* to accumulate N steadily, whereas *Distichlis* appeared oriented towards rapid, opportunistic N uptake. Based on the species' relationships between N uptake and experiment duration, an experiment lasting approximately seven weeks may not have detected a difference between *Distichlis* and *Spartina*. Our first hypothesis, that *Distichlis* would scavenge N more quickly than *Spartina*, is therefore answered affirmatively, at least when fine root mass is controlled for and with the caveat that the advantage diminishes over time.

An enhanced ability to capture short pulses of nutrients could provide a competitive advantage to *Distichlis* in conditions where N inputs are increasingly pulse-driven. *Distichlis* is understudied in salt marsh settings, but in arid terrestrial ecosystems the species has been shown to efficiently capture pulsed N delivery (James and Richards, 2005). Conversely, *Spartina* appears to have a limited ability to capture N when it is delivered by episodic rain

EPA Author Manuscript EPA Author Manuscript EPA Author Manuscript

events (Oczkowski et al., 2015), although *Spartina* does respond to seasonal to annual variation in baseline nutrient regimes (Buresh et al., 1980; Hill and Roberts, 2017). In coming decades, precipitation patterns in the northeastern US are anticipated to change in ways that augment N delivery to the coastal zone (Sinha et al., 2017). Our results suggest a shift from press- to pulse-dominated N inputs could affect salt marsh structure by benefitting *Distichlis*. Increasing dominance by *Distichlis* may enhance total N interception by salt marshes, although the difference in N interception capacity that we report is premised on NAPP differences.

The DEA rates we report are similar to values from N-fertilized plots in a low-nutrient RI salt marsh, and low (<10%) relative to RI marshes receiving high N loads (Wigand et al., 2004). Although DEA is spatially and temporally variable, it offers a reasonable upper-bound estimate of potential denitrification. Our data indicate that dominance by *Spartina* or *Distichlis* is not associated with differences in DEA, suggesting that other processes (e.g., N regime, soil redox status) are more important determinants.

4.2. ^{15}N partitioning

Our second hypothesis suggested that N would be partitioned rapidly into aboveground photosynthetic tissues in both species. During the first week after ^{15}N tracer was applied, ^{15}N moved from porewater into aboveground tissues. This is consistent with previous work showing rapid ^{15}N uptake within days of application (Hamersley and Howes, 2005; Mozdzer et al., 2014). In both species, ^{15}N concentrations and stocks were higher in aboveground tissues than belowground, as higher concentrations in aboveground tissue more than accounted for greater belowground biomass. Although ^{15}N tended to be more concentrated in *Spartina* tissues, *Distichlis* appeared to use the ^{15}N more efficiently in biomass production, leading to higher ^{15}N inventories despite generally lower ^{15}N tissue concentrations.

In addition to measuring ^{15}N accumulation in belowground tissues, we used accumulation rates to estimate belowground productivity. Belowground production is challenging to measure in salt marshes, and our data provide some suggestion that ^{15}N may be a useful tool for resolving rates of belowground production. Annualized belowground production estimates in Table 3, corresponding to annualized production rates of 2,400 and 3,000 g·m^{-2}·yr^{-1}, are higher than other estimates from the northeastern US that measured over longer periods (Anisfeld et al., 2016; Howes et al., 1985). Although our results are encouraging, the approach requires validation with independent belowground production measurements.

4.3. N uptake drivers

On a time scale of weeks, experiment duration was the strongest determinant of ^{15}N uptake rate estimates. Although medium- and long-term ^{15}N studies have been conducted to explicitly examine translocation and internal cycling (e.g., Buresh et al., 1980; White and Howes, 1994), our work is the first to intensively sample over the first month following a ^{15}N tracer application. Our ^{15}N recoveries in live plant tissue, ~20–40%, were in the lower range of values reported in the literature (Table S1), possibly related to our conservative treatment of subtracting an estimate of sorbed ^{15}N from belowground tissue concentrations.

EPA Author Manuscript

EPA Author Manuscript

EPA Author Manuscript

Our results suggest that estimates of biogeochemical process rates are dramatically affected by the passage of time between a ^{15}N pulse and the conclusion of an experiment. Experiment duration was a more powerful predictor of ^{15}N uptake rates than were primary production or plant growth rates, although the qualitative conclusion that *Distichlis* scavenged ^{15}N more rapidly than *Spartina* was consistent. We suggest that absolute rates based on partitioning studies using ^{15}N tracer should be interpreted cautiously, and where possible, in the context of potential time-related experimental biases. These biases cannot always be avoided because of the costs and logistical difficulties required to replicate experiments over multiple time spans, but experiment duration is at least an important variable to include in literature syntheses.

Supplementary Material

Refer to Web version on PubMed Central for supplementary material.

Acknowledgements

Caroline Kanaskie and Nathalie Sommer were supported by US EPA Greater Research Opportunities Fellowship Assistance Agreement nos. 91777301–0 and 91777501–0. The manuscript was improved by comments from Marty Chintala, Rose Martin, Rick McKinney, Wayne Munns, and Cathy Wigand, and three anonymous reviewers. The authors thank Rick McKinney for analytical assistance, and Russell Ahlgren and Urban Services Inc. for infrastructure support. This work was supported by the US EPA Sustainable and Healthy Communities Research Program, section 4.61.6. This report is contribution number ORD-023763 of the US EPA Office of Research and Development, National Health and Environmental Effects Research Laboratory, Atlantic Ecology Division. Although the information in this document has been funded by the US EPA, it does not necessarily reflect the views of the agency and no official endorsement should be inferred. Mention of trade names or commercial products does not constitute endorsement or recommendation for use.

7. Literature cited

Anisfeld SC and Benoit G, 1997 Impacts of flow restrictions on salt marshes: An instance of acidification. Environmental Science & Technology, 31: 1650–1657.

Anisfeld SC, Hill TD and Cahoon DR, 2016 Elevation dynamics in a restored versus a submerging salt marsh in Long Island Sound. Estuarine, Coastal and Shelf Science, 170: 145–154.

Box GE and Cox DR, 1964 An analysis of transformations. Journal of the Royal Statistical Society, Series B (Methodological), 26(2): 211–252.

Buresh RJ, DeLaune RD and Patrick WH, 1980 Nitrogen and phosphorus distribution and utilization by *Spartina alterniflora* in a Louisiana gulf coast marsh. Estuaries, 3(2): 111–121.

Craft C, Clough J, Ehman J, Joye S, Park R, Pennings S, Guo HY and Machmuller M, 2009 Forecasting the effects of accelerated sea-level rise on tidal marsh ecosystem services. Frontiers in Ecology and the Environment, 7(2): 73–78.

Fox L, Valiela I and Kinney E, 2012 Vegetation cover and elevation in long-term experimental nutrient-enrichment plots in Great Sippewissett Salt Marsh, Cape Cod, Massachusetts: implications for eutrophication and sea level rise. Estuaries and Coasts, 35(2): 445–458.

Hamersley MR and Howes BL, 2005 Coupled nitrification-denitrification measured in situ in a *Spartina alterniflora* marsh with a $^{15}NH4+$ tracer. Marine Ecology Progress Series, 299: 123–135.

Hanson A, Johnson R, Wigand C, Oczkowski A, Davey E and Markham E, 2016 Responses of *Spartina alterniflora* to multiple stressors: changing precipitation patterns, accelerated sea level rise, and nutrient enrichment. Estuaries and Coasts, 39(5): 1376–1385.

Hill TD and Roberts BJ, 2017 Effects of seasonality and environmental gradients on *Spartina alterniflora* allometry and primary production. Ecology and Evolution, 7(22): 9676–9688. [PubMed: 29187999]

EPA Author Manuscript EPA Author Manuscript EPA Author Manuscript

Hill TD, Sommer NR, Kanaskie CR, Santos EA and Oczkowski AJ, Submitted Nitrogen and carbon concentrations and stable isotope ratios: data from a ^{15}N tracer study in short-form *Spartina alterniflora* and *Distichlis spicata*. Data in Brief

Hopkinson CS and Schubauer JP, 1984 Static and dynamic aspects of nitrogen cycling in the salt marsh graminoid *Spartina alterniflora*. Ecology, 65(3): 961–969.

Howes BL, Dacey JWH and Teal JM, 1985 Annual carbon mineralization and belowground production of *Spartina alterniflora* in a New England salt marsh. Ecology, 66(2): 595–605.

Hunt R, 1990 Basic Growth Analysis: Plant Growth Analysis for Beginners Unwin Hyman, London.

James JJ and Richards JH, 2005 Plant N capture from pulses: effects of pulse size, growth rate, and other soil resources. Oecologia, 145(1): 113–122. [PubMed: 16003506]

Koop-Jakobsen K and Giblin AE, 2010 The effect of increased nitrate loading on nitrate reduction via denitrification and DNRA in salt marsh sediments. Limnology and Oceanography, 55(2): 789–802.

Levine JM, Brewer JS and Bertness MD, 1998 Nutrients, competition and plant zonation in a New England salt marsh. Journal of Ecology, 86(2): 285–292.

Lu M, Caplan JS, Bakker JD, Langley JA, Mozdzer TJ, Drake BG and Megonigal JP, 2016 Allometry data and equations for coastal marsh plants. Ecology, 97(12): 3554–3557.

Milner C and Hughes RE, 1968 Methods for the measurement of the primary production of grasslands IBP Handbook no. 6. Blackwell Scientific Publications, Oxford.

Mozdzer TJ, McGlathery KJ, Mills AL and Zieman JC, 2014 Latitudinal variation in the availability and use of dissolved organic nitrogen in Atlantic coast salt marshes. Ecology, 95(12): 3293–3303.

Oczkowski A, Wigand C, Hanson A, Markham E, Miller KM and Johnson R, 2015 Nitrogen retention in salt marsh systems across nutrient-enrichment, elevation, and precipitation regimes: a multiple-stressor experiment. Estuaries and Coasts, 39(1): 68–81.

Paerl H, Dennis R and Whitall D, 2002 Atmospheric deposition of nitrogen: Implications for nutrient over-enrichment of coastal waters. Estuaries and Coasts, 25(4): 677–693.

Paul D, Skrzypek G and Fórizs I, 2007 Normalization of measured stable isotopic compositions to isotope reference scales – a review. Rapid Communications in Mass Spectrometry, 21(18): 3006–3014. [PubMed: 17705258]

Pennings SC, Stanton LE and Brewer JS, 2002 Nutrient effects on the composition of salt marsh plant communities along the southern Atlantic and Gulf coasts of the United States. Estuaries, 25(6A): 1164–1173.

Sinha E, Michalak AM and Balaji V, 2017 Eutrophication will increase during the 21st century as a result of precipitation changes. Science, 357(6349): 405. [PubMed: 28751610]

Smart RM and Barko JW, 1980 Nitrogen nutrition and salinity tolerance of *Distichlis spicata* and *Spartina alterniflora*. Ecology, 61(3): 630–638.

Warneke S, Schipper LA, Bruesewitz DA and Baisden WT, 2011 A comparison of different approaches for measuring denitrification rates in a nitrate removing bioreactor. Water Research, 45(14): 4141–4151. [PubMed: 21696799]

White DS and Howes BL, 1994 Long-term ^{15}N-nitrogen retention in the vegetated sediments of a New England salt marsh. Limnology and Oceanography, 39(8): 1878–1892.

Wigand C, McKinney RA, Chintala MM, Charpentier MA and Groffman PM, 2004 Denitrification enzyme activity of fringe salt marshes in New England (USA). Journal of Environmental Quality, 33(3): 1144–1151. [PubMed: 15224954]

Yang WH, Traut BH and Silver WL, 2015 Microbially mediated nitrogen retention and loss in a salt marsh soil. Ecosphere, 6(1): 1–7.

EPA Author Manuscript

EPA Author Manuscript

EPA Author Manuscript

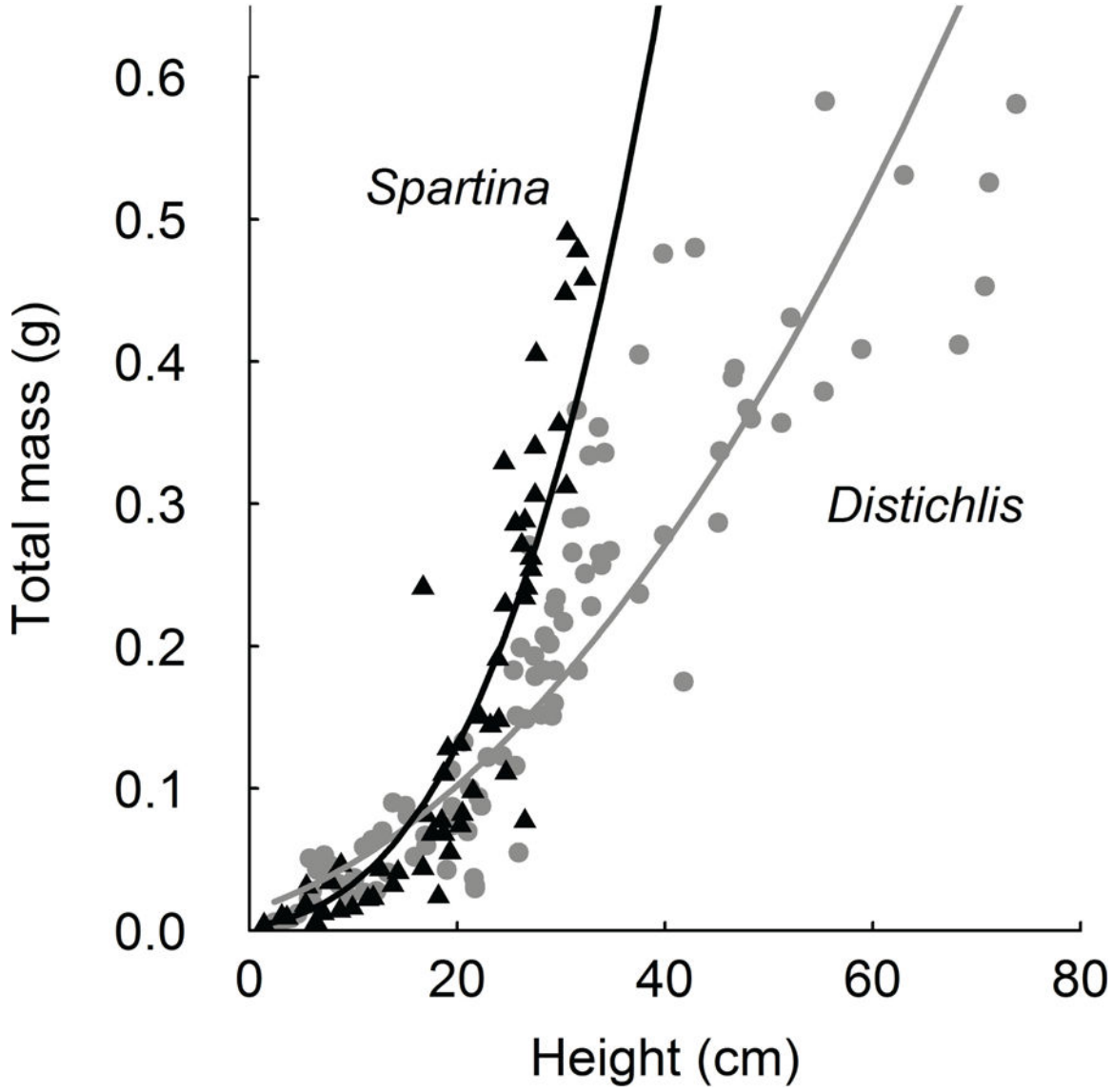

Figure 1.
Mass-height allometry for *Spartina* (black triangles) and *Distichlis* (gray circles) from Colt State Park, RI. Allometry model parameters are reported in Table 1.

EPA Author Manuscript EPA Author Manuscript EPA Author Manuscript

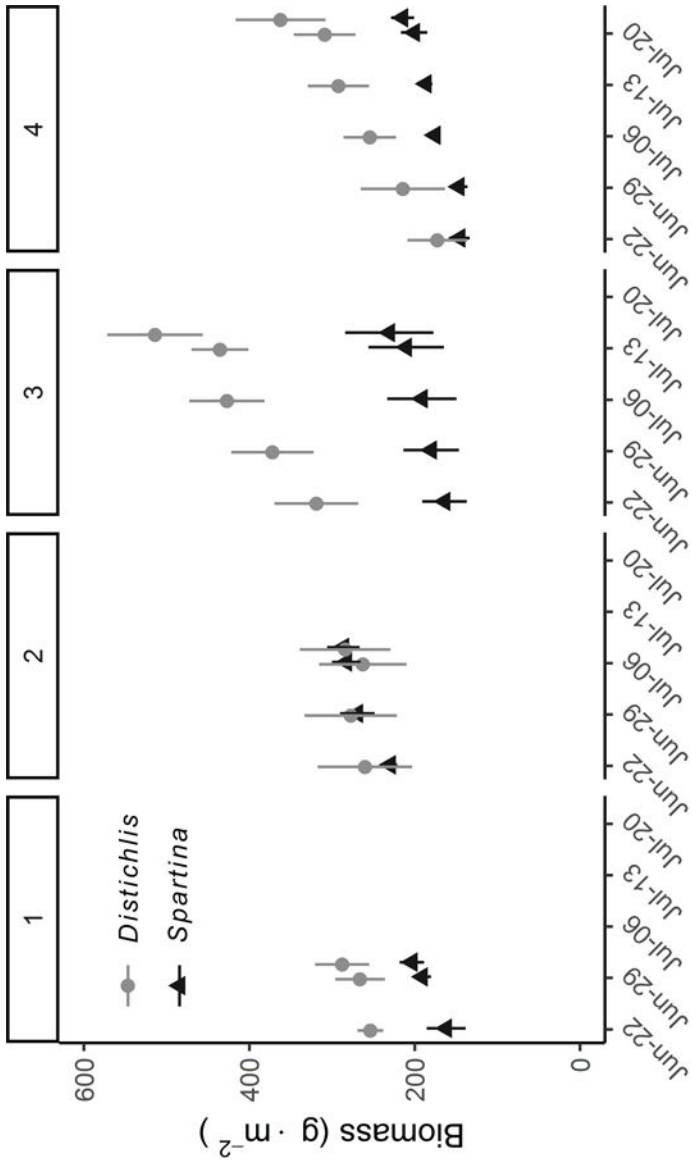

Figure 2.

Live aboveground biomass over time (mean ± SE; n = 3), for each of the four cohorts of harvested mesocosms. Points are offset for clarity; sampling dates are the same for both species.

EPA Author Manuscript

EPA Author Manuscript

EPA Author Manuscript

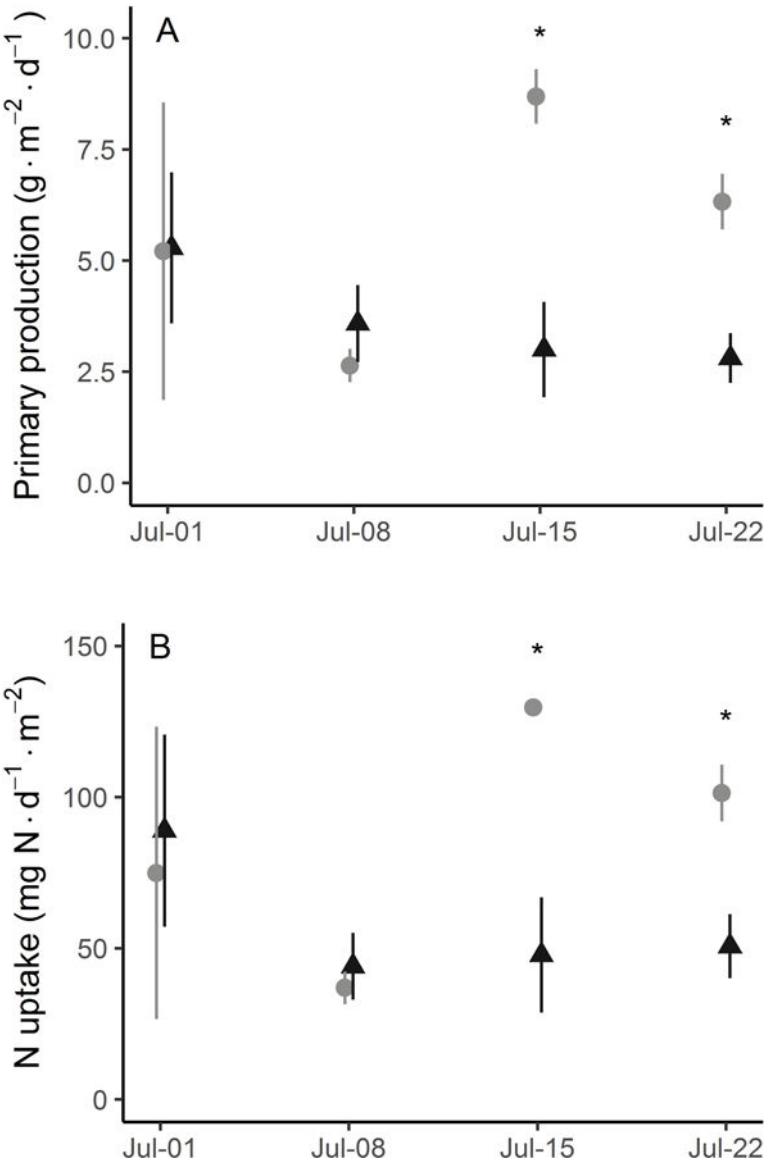

Figure 3.

Panel A: Aboveground production (mean ± SE) in each cohort of harvested mesocosms (n = 3). Gray circles are *Distichlis* and black triangles are *Spartina*. Within a harvest date, significant differences between species are indicated by asterisks (*$P < 0.05$). Panel B: Aboveground N uptake in each cohort, estimated from primary production and biomass N concentrations. The starting point for all uptake measurements was the first biomass measurement, 22 June 2016. Points are offset for clarity in both panels.

EPA Author Manuscript EPA Author Manuscript EPA Author Manuscript

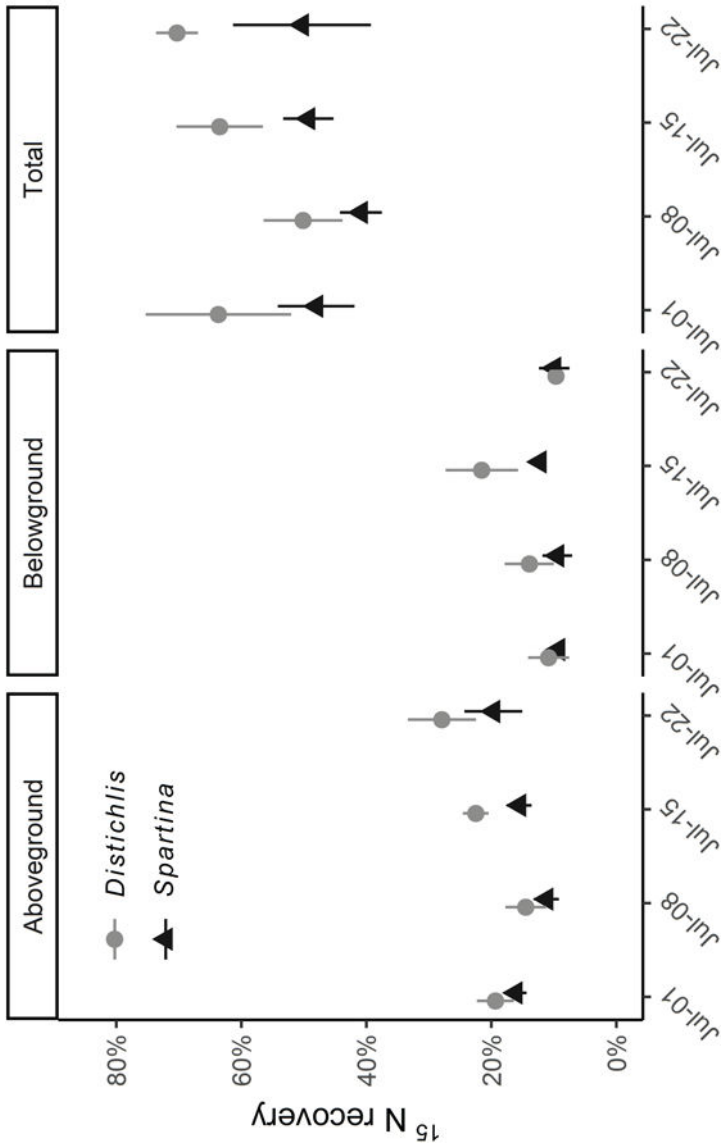

Figure 4.

^{15}N recoveries in aboveground biomass, belowground live biomass (corrected for sorption), and total (all ^{15}N recovered, including sorption, dead belowground biomass and surficial algae) at each time point, for each species (mean ± SE). Inventories were summed for all vegetative components and expressed as a percent of the ^{15}N added. Points are offset slightly for clarity.

EPA Author Manuscript

EPA Author Manuscript

EPA Author Manuscript

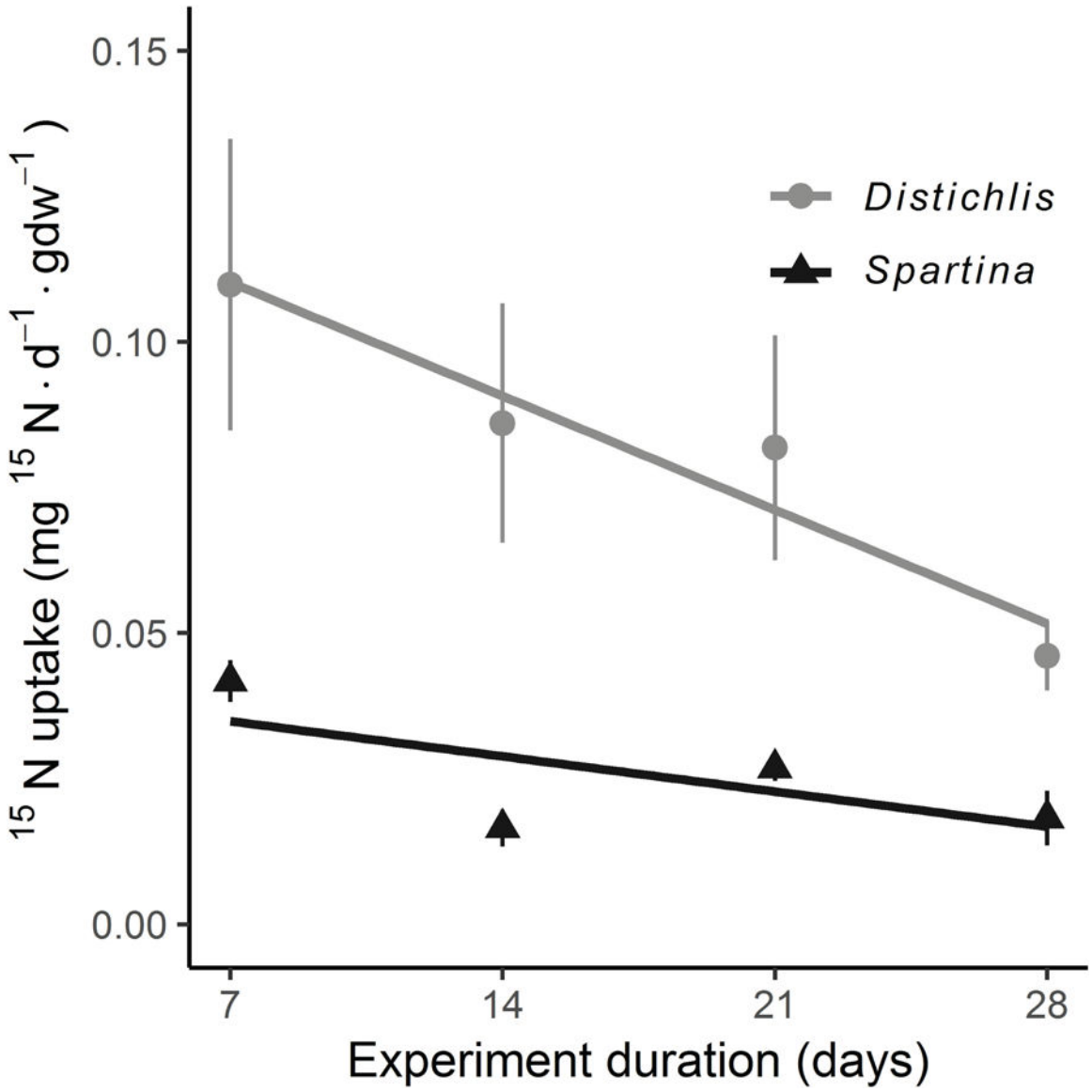

Figure 5.
Combined above- and belowground ^{15}N uptake per gram of fine root biomass (mean ± SE), as a function of experiment duration. Lines of best fit intersect at day 46.

EPA Author Manuscript

EPA Author Manuscript

EPA Author Manuscript

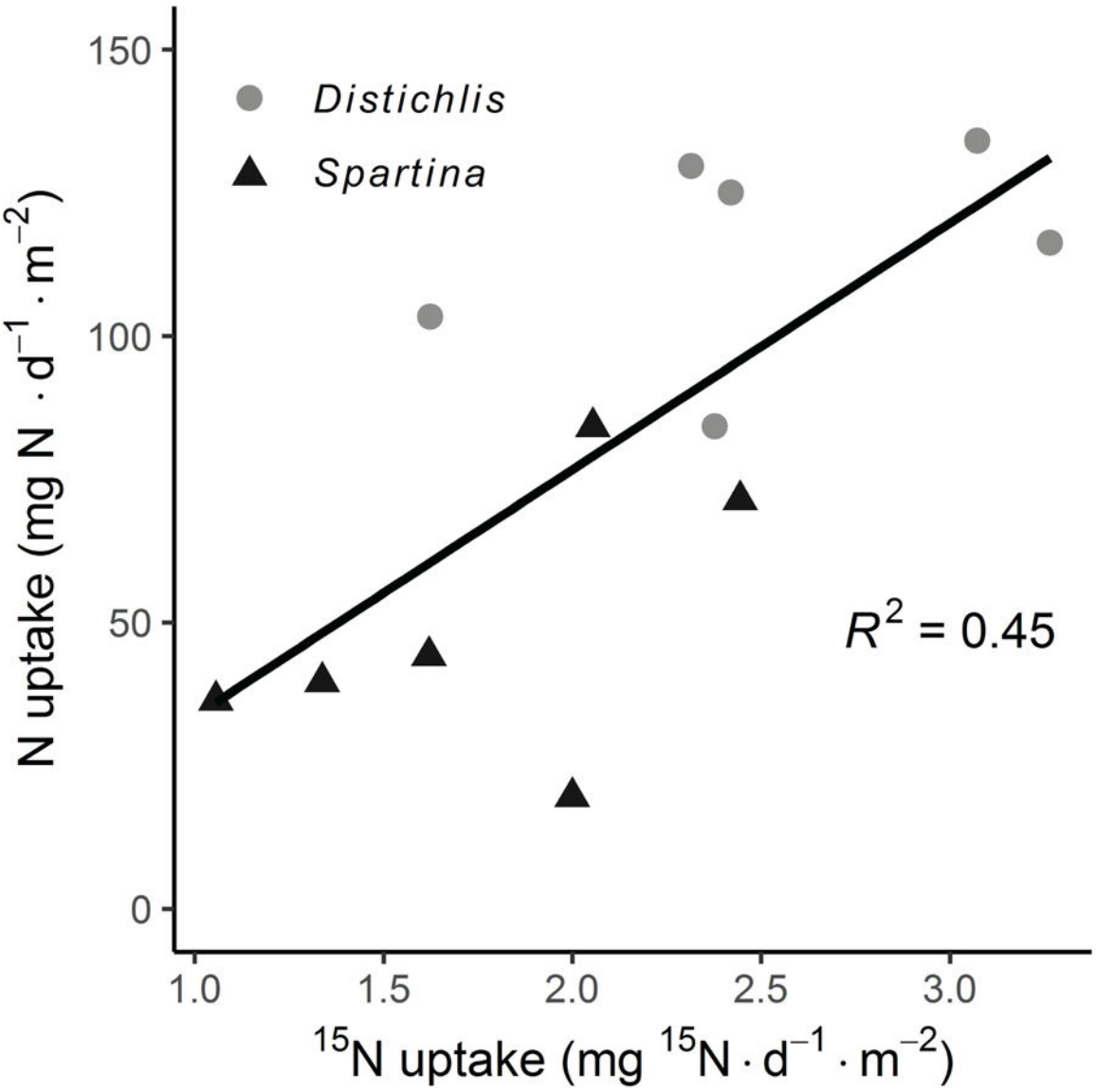

Figure 6.

Relationship between aboveground N uptake estimates calculated from ^{15}N vs. primary production rates and biomass N concentrations. Data shown are from harvests three and four weeks after ^{15}N addition; line of best fit is shown (P = 0.01; y = 43.0x – 9.4).

EPA Author Manuscript

EPA Author Manuscript

EPA Author Manuscript

Table 1.

Allometry models used to estimate masses from plant heights. Masses were estimated as $mass = (height * a + b)^{1/\lambda}$, using the intercepts (*a*), slopes (*b*), and lambda values below.

Species	Intercept	Slope	λ	R^2	n
Distichlis spicata	0.118	0.010	0.50	0.84	95
Spartina alterniflora (short-form)	0.137	0.019	0.33	0.96	75

EPA Author Manuscript

EPA Author Manuscript

EPA Author Manuscript

Table 2.

Excess ^{15}N concentrations and ^{15}N inventories in live plant tissues (mean ±SE in parentheses; n = 12). Excess ^{15}N includes a sorption correction for belowground tissue. For each tissue type, asterisks indicate significant differences between species (*$P < 0.05$; **$P < 0.01$; ***$P < 0.001$; Welch's two-sample t-test). Inventories reflect recovery of the 243 mg $^{15}N \cdot m^{-2}$ added.

	Excess ^{15}N (atom %)		^{15}N (mg $^{15}N \cdot m^{-2}$)	
Tissue	***Spartina***	***Distichlis***	***Spartina***	***Distichlis***
Leaf	1.40 (0.13)*	0.99 (0.09)*	25.0 (3.5)	24.9 (4.0)
Stem	1.66 (0.13)**	1.14 (0.11)**	12.9 (1.1)***	26.3 (2.3)***
Fine root	0.65 (0.06)*	0.87 (0.07)*	9.0 (0.9)*	6.2 (0.7)*
Coarse root	0.48 (0.10)	0.56 (0.17)	5.1 (0.7)	6.7 (2.4)
Rhizome	0.45 (0.06)*	0.28 (0.04)*	10.8 (1.6)*	21.0 (3.5)*
Total aboveground	1.49 (0.11)**	1.07 (0.09)**	37.9 (3.7)	51.2 (5.2)
Total belowground	0.51 (0.05)*	0.36 (0.05)*	24.8 (2.1)	34.0 (5.3)
Above + Belowground	0.85 (0.07)**	0.60 (0.04)**	62.8 (5.0)*	85.2 (7.5)*

EPA Author Manuscript

EPA Author Manuscript

EPA Author Manuscript

Table 3.

Mean (SE in parentheses) N uptake, and primary production from mesocosms harvested 3–4 weeks after ^{15}N application, and denitrification potentials measured two weeks after application. For each parameter, asterisks indicate significant differences between species (*** $P < 0.001$, Welch's two-sample t-test). All units are expressed per m^2 per day.

Species	Total N uptake (mg N)		Primary production (g dw)		Denitrification potential (mg N)	Unamended N_2O+N_2 flux (mg N)
	Below[1]	Above	Below[1]	Above		
Distichlis	62.2	115.5***	7.2	7.5***	99.4	39.4
	(20.5)	(7.7)	(5.9)	(0.7)	(32.4)	(23.0)
Spartina	39.6	49.2***	5.9	2.9***	65.4	8.9
	(7.1)	(9.8)	(1.3)	(0.5)	(23.6)	(1.1)

[1] Estimated as described in equations 3 and 4.